



# Penetration into low-density media: In situ observation of penetration process of various projectiles

Toshihiko Kadono<sup>a,\*</sup>, Rei Niimi<sup>b</sup>, Kyoko Okudaira<sup>c</sup>, Sunao Hasegawa<sup>d</sup>,  
Makoto Tabata<sup>d,e</sup>, Akira Tsuchiyama<sup>b,f</sup>

<sup>a</sup> School of Medicine, University of Occupational and Environmental Health, Yahata, Kitakyusyu 807-8555, Japan

<sup>b</sup> Department of Earth and Space Science, Osaka University, Toyonaka, Osaka 560-0043, Japan

<sup>c</sup> Office for Planning and Management, The University of Aizu, Aizuwakamatsu, Fukushima 965-8580, Japan

<sup>d</sup> Institute of Space and Astronautical Science, Japan Aerospace Exploration Agency, Sagami-hara, Kanagawa 252-5210, Japan

<sup>e</sup> Department of Physics, Chiba University, Inage, Chiba 263-8522, Japan

<sup>f</sup> Division of Earth and Planetary Sciences, Kyoto University, Sakyo-ku, Kyoto 606-8502, Japan

## ARTICLE INFO

### Article history:

Received 7 February 2012

Revised 23 August 2012

Accepted 23 August 2012

Available online 6 September 2012

### Keywords:

Comets

Impact processes

Interplanetary dust

## ABSTRACT

In order to understand the penetration process of projectiles into lower-density targets, we carry out hypervelocity impact experiments using low-density ( $60 \text{ mg cm}^{-3}$ ) aerogel targets and various types of projectiles, and observe the track formation process in the targets using a high-speed camera. A carrot shaped track, a bulbous, and a “hybrid” one consisting of bulbous and thin parts, are formed. The results of the high-speed camera observations reveal the similarity and differences on the temporal evolution of the penetration depth and maximum diameter of these tracks. At very early stages of an impact, independent of projectile type, the temporal penetration depth is described by hydrodynamic models for the original projectiles. Afterward, when the breakup of projectiles does not occur, intact projectiles continue to penetrate the aerogels. In the case of the breakup of projectiles, the track expands with a velocity of about a sound velocity of the aerogel at final stages. If there are large fragments, they penetrate deeper and the tracks become a hybrid type. The penetration of the large fragments is described by hydrodynamic models. Based on these results, we discuss the excavation near the impact point by shock waves.

© 2012 Elsevier Inc. All rights reserved.

## 1. Introduction

Hypervelocity impact experiments on very low-density materials have been carried out to extend the cratering experiments (e.g., Cannon and Turner, 1967; Fechtig et al., 1980; Werle et al., 1981; Love et al., 1993; Trucano and Grady, 1995) and to develop and calibrate the instruments for intact capture of interplanetary dust samples using foams (e.g., Ishibashi et al., 1990; Tsou, 1990) and for aerogels (e.g., Barrett et al., 1992; Hörz et al., 1993, 1998, 2009; Burchell et al., 1999, 2001, 2008, 2009; Kitazawa et al., 1999; Niimi et al., 2011, 2012). These previous studies indicate that the impacts between high-density projectiles and low-density targets generate “penetration tracks”: track diameter is small at the entrance (= impact point), then increases with depth, takes a peak, and decreases (this qualitative feature is common for any track). For more quantitative description, the depth  $L$  and the maximum diameter  $D_m$  of final tracks are often measured as a function of the parameters varied in the experiments such as, projectile

density  $\rho_p$ , projectile diameter  $D_p$  (radius  $R_p$ ), projectile and target strengths, target density  $\rho_t$ , and impact velocity  $v_0$ . The features about  $L/D_p$  and  $D_m$  suggested by previous various experiments with low-density targets are roughly summarized as follows:  $L/D_p$  increases with  $v_0$ , and takes a peak, then decreases (e.g., Fechtig et al., 1980; Werle et al., 1981; Ishibashi et al., 1990; Tsou, 1990; Barrett et al., 1992; Kitazawa et al., 1999; Burchell et al., 2001; Hörz et al., 2009), and is scaled by  $\rho_p/\rho_t$  (e.g., Barrett et al., 1992; Hörz et al., 1993; Love et al., 1993; Burchell et al., 1999, 2009; Niimi et al., 2011, 2012), and  $D_m$  is proportional to  $D_p$  regardless of  $\rho_p/\rho_t$  and proportional to  $v_0$  (e.g., Ishibashi et al., 1990; Kitazawa et al., 1999; Burchell et al., 2008; Niimi et al., 2012).

Several models have been proposed on the penetration depth (e.g., Anderson and Ahrens, 1994; Trucano and Grady, 1995; Westphal et al., 1998; Kadono, 1999; Domínguez et al., 2004; Kadono and Fujiwara, 2005; Trigo-Rodríguez et al., 2008; Domínguez, 2009; Coulson, 2009a,b; Niimi et al., 2011). Most models suggest that projectiles receive the hydrodynamic force  $(C_d/2)\rho_t v^2 S$ , where  $C_d$ ,  $v$ , and  $S$  are the drag coefficient, instantaneous velocity, and the cross-sectional area, respectively, for  $v$  higher than the sound velocity of target materials. Thus, the feature about the depth  $L$  is relatively understood (e.g., the feature that  $L/D_p$  increases with  $v_0$ ,

\* Corresponding author.

E-mail address: [kadono@med.uoeh-u.ac.jp](mailto:kadono@med.uoeh-u.ac.jp) (T. Kadono).

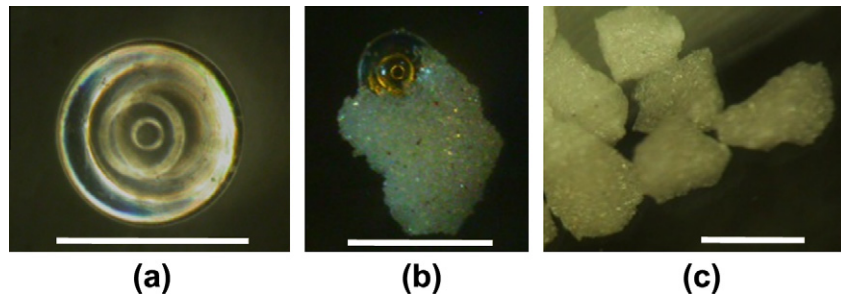


**Fig. 1.** Projectiles used in this experiment. The scale bar in each figure indicates 500  $\mu\text{m}$ . (a) Projectile (A), SLG with 491  $\mu\text{m}$ . (b) Projectile (B), a sintered mixture of SLG ( $\sim 300 \mu\text{m}$ ) and small silica beads ( $< 20 \mu\text{m}$ ) with a bulk diameter of  $\sim 500 \mu\text{m}$ . (c) Projectile (C), sintered small silica aggregates with a bulk diameter of  $\sim 300 \mu\text{m}$ .

takes a peak, and then decreases, is explained such that, at low  $v_0$ , projectiles are intact and  $L/D_p$  indicates a logarithmic increase with  $v_0$ , then at a critical  $v_0$ , the breakup of projectiles occurs, and, as  $v_0$  increases, the largest fragment becomes smaller and  $L/D_p$  decreases). On the other hand, there are a relatively small number of researches on the growth of track diameter (Westphal et al., 1998; Kadono, 1999; Domínguez et al., 2004; Trigo-Rodríguez et al., 2008; Coulson, 2009b; Domínguez, 2009). As the mechanisms of the expansion of the track diameter, shock waves (Domínguez et al., 2004), thermal effects (Kadono, 1999; Coulson, 2009b; Domínguez, 2009), and fragmentation of projectiles (Kadono, 1999; Trigo-Rodríguez et al., 2008) have been considered. However, among the common features for any track about track diameter, in particular, the track profile near the entrance is still not clear.

To understand the track diameter evolution, we focus on the similarities and differences on the formation process of various tracks, based on the in situ observation in laboratory experiments. There have been a few attempts so far for in situ observation of penetration process into low-density materials, such as breakwire (Tsou, 1990), magnetic pickup (Tsou, 1990), X-ray shadow graphs (Tsou, 1990; Trucano and Grady, 1995) and an optical high-speed camera with aerogel targets (Niimi et al., 2011). However, these results mainly consider the penetration depth of hard projectiles. In this paper, we used three types of projectiles and observed the track formation process (the track length, the growth rate of bulbous tracks, and the position of the maximum diameter), using a high-speed camera as a function of time. Based on the results and the previous models, we briefly discuss the track formation process.

## 2. Experiments

Impact experiments were carried out using a two-stage hydrogen gun at Institute of Space and Astronautical Science, JAXA. We used three types of projectiles: (A) a spherical soda-lime-glass (SLG) with a diameter of 491  $\mu\text{m}$  and a density of  $2.5 \text{ g cm}^{-3}$  (Fig. 1a), (B) a sintered mixture of small silica (the size of the constituting silica particles less than 20  $\mu\text{m}$ ) and a large SLG particle ( $\sim 300 \mu\text{m}$ ) with a bulk diameter of  $\sim 500 \mu\text{m}$  and a bulk density of  $\sim 1.4 \text{ g cm}^{-3}$  (Fig. 1b), and (C) sintered small silica ( $< 20 \mu\text{m}$ ) aggregates with a bulk diameter of  $\sim 300 \mu\text{m}$  and a bulk density of  $\sim 1.9 \text{ g cm}^{-3}$  (Fig. 1c). In the cases of Projectiles (A) and (B), a single particle was launched using nylon cylindrical sabots (Kawai et al., 2010), while several particles were simultaneously accelerated using split-type sabots in the case of Projectile (C). The impact velocity was set to be  $\sim 4 \text{ km s}^{-1}$ . Targets were silica aerogel with a density of  $60 \text{ mg cm}^{-3}$  made by Panasonic Electric Works Co., Ltd. in all cases. Penetration process data was taken with a high-speed video camera (HyperVision HPV-1 by Shimadzu Corp.). The experimental conditions are summarized in Table 1.

## 3. Results

### 3.1. Track morphology

Fig. 2 shows the consecutive images of penetration process. (a) Projectile (A), SLG. The time interval between each frame is 8  $\mu\text{s}$  from the first to the 11-th frame and 80  $\mu\text{s}$  from the 11th to the 15th one. (b) Projectile (B), the mixture of SLG and small silica. The time interval between each frame is 8  $\mu\text{s}$  from the first to the 8th frame and 80  $\mu\text{s}$  from the 8th to the 10th frame. (c) Projectile (C), small silica aggregates. The time interval is 4  $\mu\text{s}$  for all frames. The projectiles come from left. In Fig. 2a, as described in Niimi et al. (2011), Projectile (A) SLG made a slender carrot shaped track. Recovered terminal grain is shown in Fig. 3a. The grain shape is spherical and its diameter is the same as that before the impact, though the front hemisphere is slightly covered with melted silica aerogels. Projectile (B) SLG + small silica made a “hybrid” track, which consists of bulbous and thin (indicated by an arrow in Fig. 2b) parts. The thin part appears at the second frame and stops at about 6th or 7th frame, while the bulbous part still expands in its depth and diameter after the thin part stops. The terminal grain was recovered from the tip of the thin part (Fig. 3b). This is the maximum fragment with a size of 150–200  $\mu\text{m}$  in this track. This fact supports the idea that the maximum fragment makes the thin part of such hybrid type tracks (e.g., Kadono, 1999; Iida et al., 2010). It is noted that the recovered terminal grain is not the originally included SLG with 300  $\mu\text{m}$ . The SLG with 300  $\mu\text{m}$  may be detached before the impact or be broken at the impact. For Projectile (C) small silica aggregates, in Fig. 2c, there are two tracks. It looks that only bulbous part is made. The expansion velocities of the depth and diameter are similar in each track.

### 3.2. Penetration depth

In Fig. 4a, the track length from the entrance for SLG is plotted as a function of time. We define time 0 as the previous frame before an impact track clearly begins to be observed. For comparison, the penetration depth as a function of time calculated by a model by Niimi et al. (2011) (hereafter “Niimi model”) is also plotted as a bold curve for the same impact condition (the parameters such as the drag coefficient  $C_d$  and target strength  $P_c$  are set to be the same values as those in Niimi et al. (2011), 1.1 and 1.9 MPa, respectively). The curve is adjusted to pass the first experimental data point. The curve agrees well with the experimental result, though there is a slight difference, which is already pointed out in Niimi et al. (2011).

In Fig. 4a, the position of the tip of the thin part in the case of Projectile (B), the mixture projectile, is also plotted after the thin part appears in the second frame. Using Niimi model, we calculate the temporal track length for Projectile (B) with the original projec-

Download English Version:

<https://daneshyari.com/en/article/10701426>

Download Persian Version:

<https://daneshyari.com/article/10701426>

[Daneshyari.com](https://daneshyari.com)